EDGE ARTICLE

Check for updates

A tin analogue of propadiene with cumulated C=Sn double bonds†

Koh Sugamata, [ID] * Teppei Asakawa and Mao Minoura [ID]

The synthesis, structure, and properties of a stable, linear 2-stannapropadiene are reported. The identical C=Sn bonds in this 2-stannapropadiene are the shortest hitherto reported C–Sn bonds. This 2-stannapropadiene features a ^{119}Sn NMR signal at 507 ppm for the central tin atom, indicative of an unsaturated Sn^{4+} oxidation state. Due to the inert-pair effect, the tin atom displays a pronounced preference for the +2 oxidation state over the +4 oxidation state. Nevertheless, by employing silyl substituents, it is possible to disrupt the inert-pair effect, leading to the formation of an isolable 2-stannapropadiene with a linear structure centered on a Sn^{4+} atom. Treatment of this 2-stannapropadiene with $SnBr_2$·dioxane resulted in the formation of a novel four-membered cyclic 1,1-dibromo-1,3-distannetane, which was subsequently reduced to afford the corresponding stable four-membered cyclic bis(stannylene).

Introduction

Zero-valent, di-coordinated group-14-element compounds, the so-called called ylidones, have been extensively studied over the last decade, and C, Si, Ge, Sn, and Pb analogues have already been reported.[1–10] Ylidones represent one of the isomers of the heavier analogues of allenes; however most ylidones have been characterized as zero-valent compounds (E^0) rather than allenes (E^{4+}). The first 1-metallaallenes reported were the Si analogues (**A** in Fig. 1) synthesized by West *et al.* in 1993 and the Ge analogues (**B** and **C**) independently synthesized in 1998 by West as well as Tokitoh and Okazaki.[11–13] Subsequently, the synthesis, reactivity, and unique properties of their analogues were investigated.[14–18] Interestingly, an attempted synthesis of 1-stannapropadiene (**D**) along a similar synthetic route was reported by Escudié in 2004; however this led to an unprecedented stable distannirane (**E**) *via* a [2 + 1] cycloaddition between a transient stannylene and a 1-stannapropadiene (**D**).[19] This was the first tangible piece of evidence for the transient formation of a 1-stannapropadiene. In contrast, there is only one example each for the Si, Ge and Sn 2-metallaallene analogues (**F**, **G**, and **H**) using the same diphenythiophosphinoyl groups ($Ph_2(S)P$–) on the terminal carbon atoms of their allene moieties.[20–22] Importantly, the structural features of these compounds are not consistent with classical allene character due to the coordination of the sulfur atom in the substituents to the central metal atoms. Accordingly, tin analogues of allenes

with cumulative C=Sn π-bonds have remained elusive thus far. Earlier studies have reported on the isolation and characterization of a linear 2-germapropadiene (1_{Ge}) by using bulky silyl substituents.[23] A single-crystal X-ray electron-density-distribution (EDD) analysis of 1_{Ge} allowed us to obtain the differential electron-density map of 1_{Ge}, which suggested two orthogonal π-bonds for the C=Ge=C moiety. Thus, 1_{Ge} represents the first example of a stable, structurally characterized germanium-centered heteroallene with a linear structure. Furthermore, the reactivity of 1_{Ge} is consistent with that of an allene rather than a tetrylone. To further investigate the properties of the corresponding 2-stannapropadiene, ^{119}Sn NMR
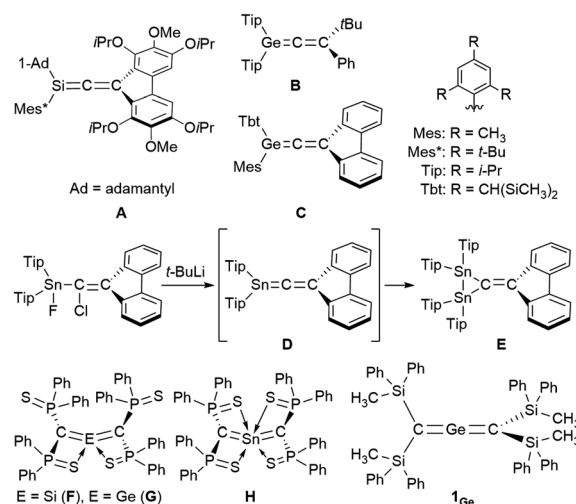
Department of Chemistry, College of Science, Rikkyo University, 3-34-1 Nishi-Ikebukuro, Toshima-ku, Tokyo 171-8501, Japan. E-mail: sugamata@rikkyo.ac.jp

Fig. 1 Heteroallenes that contain heavier group-14 atoms and related compounds.

spectroscopy should offer a useful diagnostic tool for the determination of the electronic structure of the target compound. Herein, we report the synthesis and properties of a 2-stannapropadiene ($\mathbf{1_{Sn}}$). The combined results of X-ray crystallographic and NMR spectroscopic analyses suggest that $\mathbf{1_{Sn}}$ exists as an allene-type structure in the solid state and in solution. The linear structure of $\mathbf{1_{Sn}}$ with cumulative C=Sn double bonds was confirmed by X-ray crystallography for the first time.

Results and discussion

As previously reported, $\mathbf{1_{Ge}}$ can be obtained from the reaction between bis(silyl)carbenoid R^{Si}_2CLiBr, which is generated *in situ* from the reaction of $R^{Si}_2CBr_2$ with *t*-BuLi (2 eq.) in THF at -95 °C, and $GeCl_2 \cdot dioxane$ (1.0 eq.) at -95 °C.[24] After removal of the generated LiBr and recrystallization from hexane and benzene, $\mathbf{1_{Ge}}$ can be obtained as pale-yellow crystals in 50% yield. The tin analogue ($\mathbf{1_{Sn}}$) was prepared in a similar manner, *i.e.*, the bis(-silyl)carbenoid was generated using the previously outlined procedure, and $SnCl_2 \cdot dioxane$ (0.33 eq.) was added at low temperature (Scheme 1). After removal of all inorganic salts, recrystallization from hexane and benzene afforded 2-stannap-ropadiene ($\mathbf{1_{Sn}}$) as yellow crystals in 57% yield. While $\mathbf{1_{Ge}}$ forms the corresponding cyclic thermal isomer quantitatively in solution after 2 h at 60 °C upon 1,3-migration of the phenyl group, $\mathbf{1_{Sn}}$ does not undergo thermal decomposition, not even in solution after 12 h at 100 °C.

The characterization of $\mathbf{1_{Sn}}$ was accomplished using multi-nuclear NMR, ultraviolet-visible (UV-vis), and infrared (IR) spectroscopy as well as mass spectrometry and single-crystal X-ray diffraction analysis (Fig. 2). The solid-state structure of $\mathbf{1_{Sn}}$ exhibits D_{2d} symmetry with a linear C–Sn–C moiety (C–Sn–C angle: 178.06(6)°) and almost identical C–Sn bonds (C1–Sn1: 1.9787(15) Å; C2–Sn1: 1.9827(16) Å). These C–Sn bonds represent some of the shortest among the hitherto structurally characterized organotin species with C=Sn double bonds such as stannenes [2.003(5)–2.073(10) Å][25–29] and are significantly shorter than those of a previously reported base-stabilized 2-stannapropadiene (2.063(2) Å).[20] Furthermore, the allenic moiety of the base-stabilized 2-stannapropadiene is slightly bent (171.1(1)°) with pyramidal carbon atoms (ΣC_{allene}: 354.6°). In contrast, the two terminal carbon atoms of $\mathbf{1_{Sn}}$ are almost planar ($\Sigma C1$: 359.6°; $\Sigma C2$: 359.8°), indicating that the structural properties of $\mathbf{1_{Sn}}$ are considerably different from those of the base-stabilized 2-stannapropadiene. The C1–Si1–Si2 and C2–Si3–Si4 planes slightly deviate from a perpendicular
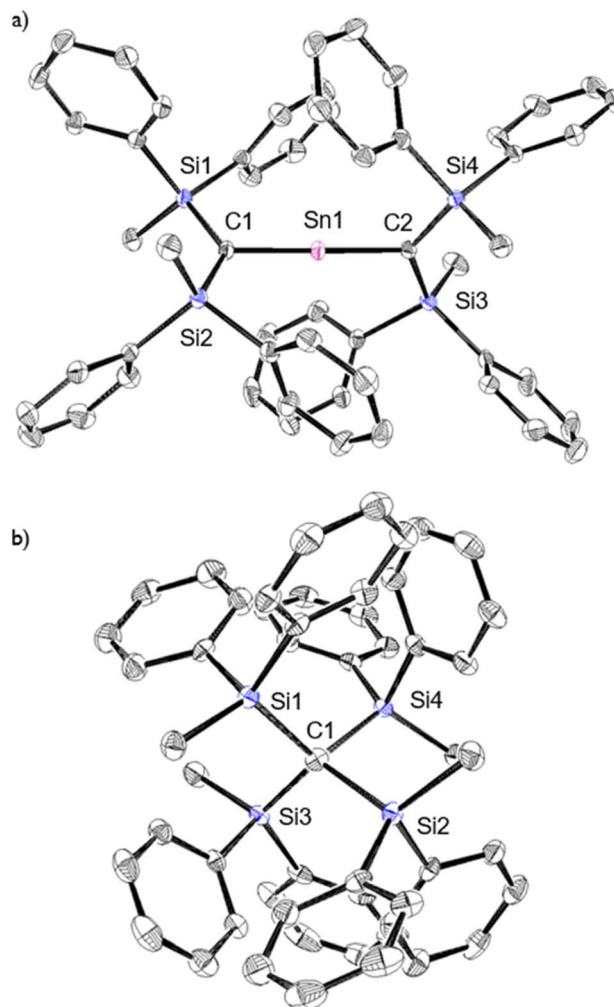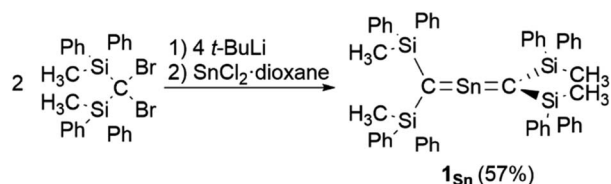

Scheme 1 Synthesis of 2-stannapropadiene $\mathbf{1_{Sn}}$.

Fig. 2 (a) Top and (b) side views of the molecular structure of $\mathbf{1_{Sn}}$ in the crystalline state with thermal ellipsoids at 50% probability; hydrogen atoms are omitted for clarity. Selected bond lengths [Å] and angles [°] for $\mathbf{1_{Sn}}$: C1–Sn1: 1.9787(15), C2–Sn1: 1.9827(16), C1–Si1: 1.8410(16), C1–Si2: 1.8336(16), C2–Si3: 1.8423(16), C2–Si4: 1.8428(16), C1–Sn–C2: 178.06(6), Si1–C1–Si2: 130.90(9), Si1–C1–Sn1: 114.62(8), Si2–C1–Sn1: 114.07(8), Si3–C2–Si4: 133.33(9), Si3–C2–Sn1: 112.17(8), and Si4–C2–Sn1: 114.29(8).

arrangement relative to each other (79.9°), probably due to the steric repulsion among the silyl groups.

The molecular structure of $\mathbf{1_{Sn}}$ was further examined using theoretical calculations. The structural characteristics of $\mathbf{1_{Sn}}$, which were optimized at the B3PW91-D3(bj)/Def2TZVP level for Sn and the 6-311G(2d,p) level for the rest of the atoms, are in good agreement with those obtained experimentally (Fig. S45†), *i.e.*, the linear geometry of the C=Sn=C moiety (C–Sn–C = 180.0°) and the two C–Sn bond lengths (1.959 Å) are close to the values obtained from the XRD analysis (C1–Sn1: 1.9787(15) Å; C2–Sn1: 1.9827(16) Å). The introduction of H_3Si substituents on the 2-stannapropadiene ($\mathbf{1_{Sn}}^{H3Si}$) resulted in an optimized linear structure, whereas the H-, H_3C-, and H_2N-substituted 2-stan-napropadienes $\mathbf{1_{Sn}}^{H}$, $\mathbf{1_{Sn}}^{H3C}$, and $\mathbf{1_{Sn}}^{H2N}$ exhibit bent structures, suggesting that the presence of silyl substituents on the terminal carbon affect the linear C=Sn=C structure of $\mathbf{1_{Sn}}$.

That is, the π-electron accepting ability of the silyl groups on the terminal carbons would be crucial for the formation of the linear structure of 2-stannapropadiene. Apeloig and co-workers have reported the synthesis of a tetrasilyl-substituted distannene with a non-twisted structure that exhibits an almost perfect planar geometry due to the suitable steric effect and the silyl substituent effect.[30] The frontier Kohn–Sham orbitals of 1_{Sn} provided further information on the nature of the cumulated C=Sn bonds. The HOMO (π), HOMO−1 (π), LUMO+1 (π*), and LUMO+2 (π*) of 1_{Sn} reveal features typical of compounds with a linear allene-type structure (Fig. 3b). A natural bond orbital (NBO) analysis of the optimized structure of 1_{Sn} showed two C–Sn π-bonds that consist of almost pure 5p orbitals of the tin atom and 2p orbitals of the carbon atoms on the allene moiety.[31] The calculated natural-population-analysis (NPA) charges on the tin atom (+2.06) and on each of the terminal carbon atoms (−1.95) indicate a stronger polarization in the allene moiety of 1_{Sn} compared to that of the germanium derivative 1_{Ge} (Ge: +1.76; C: −1.86).[23]

To investigate the multiple-bond character of 1_{Sn} by vibrational spectroscopy, we recorded the IR spectrum (KBr, pellet) of 1_{Sn} in the solid state (Fig. S53†). The C=Sn=C asymmetric stretching

frequency of 1_{Sn} is observed at 930 cm^{-1} and the assignment of this IR shift was supported by DFT calculations (925 cm^{-1}). This frequency is slightly lower than the C=Ge=C asymmetric stretching frequency of 1_{Ge} (973 cm^{-1}) and significantly lower than the C=C=C asymmetric stretching frequency of 1,1,3,3-tetrakis(trimethylsilyl)allene (1870 cm^{-1}).[32,33] It can thus be concluded that the frequency of the stretching vibration reflects the bond strength of the allene moieties. In the ^{1}H NMR spectrum of 1_{Sn} in C_6D_6, the signal for the protons of the methyl groups was observed as a sharp singlet at 0.39 ppm, indicating a highly symmetric structure for 1_{Sn} in solution. The resonance for the carbon nuclei of the terminal carbons in the allene moiety was observed at 107 ppm, i.e., shifted slightly down-field relative to those of previously reported 2-germapropadiene 1_{Ge} (86 ppm) and tetrakis(trimethylsilyl)allene (64 ppm).[32,33] Moreover, the ^{119}Sn NMR signal for the tin atom was observed at 507 ppm in C_6D_6, indicating unsaturated Sn^{4+} character, similar to those of the stable stannenes (270–835 ppm) and stannaaromatic compounds (264–491 ppm) shown in Fig. 4.[34–37] However, this value is significantly lower than those of previously reported stannylones ((−1147)–64 ppm), which are zero-valent tin species, and higher than those of kinetically stabilized stannylenes (2235–2323 ppm), which are Sn^{2+} species.[38,39] The central tin atom of a tris-tannaallene has been observed at 2233 ppm due to the considerable unsaturated character that is similar to that in stannylenes, and a stereochemically active lone pair of electrons.[40] In contrast to the resonance of the ^{119}Sn nucleus in the base-stabilized 2-stannapropadiene (−401 ppm), the resonance of 1_{Sn} is characteristic for an unsaturated tin compound.[21] Moreover, the ^{119}Sn NMR signal of 1_{Sn} in THF at 20 °C was observed as a broadened peak at 497 ppm. With decreasing temperature, this signal gradually shifts to a higher field (Fig. S38†), suggesting a dynamic process. At −50 °C, the signals were observed at 475 ppm and 362 ppm. Gauge-independent atomic orbital (GIAO) ^{119}Sn NMR calculations for the optimized structure of 1_{Sn} afforded a value of 849 ppm. When the solvent effect for THF was considered using the SCRF method, no significant shift in the signal was observed (847 ppm). However, for 1_{Sn}·THF, wherein one molecule of THF is coordinated to the central tin atom, a significant signal shift to 539 ppm was observed. The optimized structure of 1_{Sn}·THF
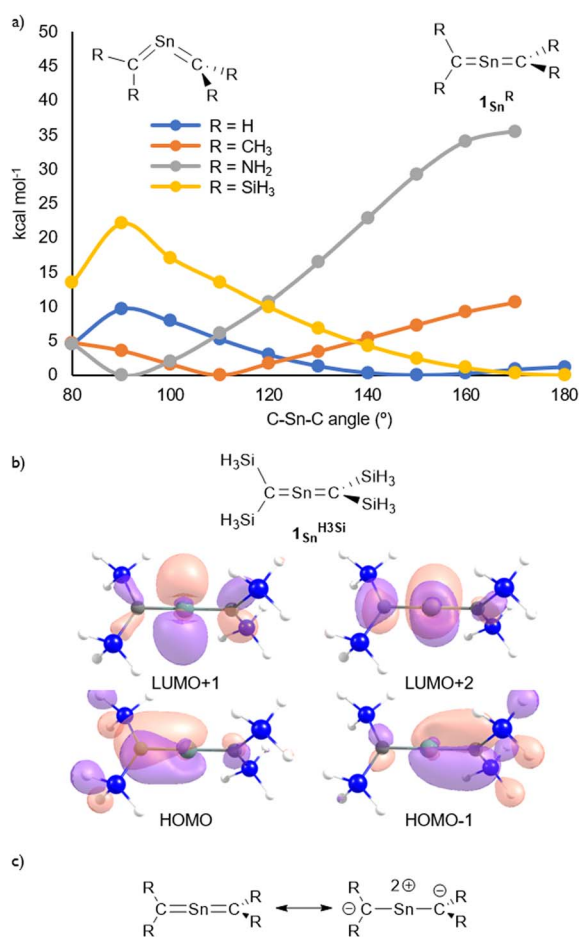

Fig. 3 (a) Optimized structures of 2-stannapropadienes calculated at the B3PW91-D3(bj)/Def2TZVP level for Sn and the 6-311G(2d,p) level for the remaining atoms. (b) Kohn–Sham orbitals of 1_{Sn}^{H3Si}. (c) Canonical resonance structures of linear 2-stannapropadienes.
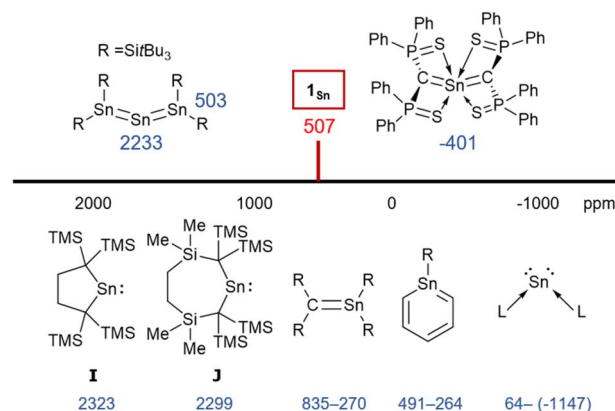

Fig. 4 ^{119}Sn NMR chemical shifts of 1_{Sn} and related compounds.

revealed a bent C–Sn–C moiety (Fig. S46†), and this distortion in the molecular geometry around the tin atom would feasibly account for the observed changes of the chemical shifts. To investigate the dynamics of 1_{Sn} in THF, variable-temperature (VT) ^{1}H NMR experiments were carried out. As shown in Fig. S37,† the methyl protons of 1_{Sn} were observed as a broadened peak (0.20 ppm) at room temperature. At −50 °C, these protons were observed as two independent sharp singlet signals (0.31/0.16) with a 1 : 3 ratio. However, at 40 °C, all methyl protons appeared as a sharp singlet, suggesting rapid dissociation of the coordinated THF molecule from the central tin atom of 1_{Sn}.

The ultraviolet-visible (UV-vis) spectrum of 1_{Sn} in benzene exhibits an absorption maximum at $\lambda_{max} = 328$ nm (ε 8000 dm³ mol⁻¹ cm⁻¹), indicating the presence of π-bonding without conjugation between the two C=Sn double bonds (Fig. 5). This value differs significantly from those of our previously reported R^{Si}_2C=Ch=CR^{Si}_2 compounds (Ch = S: 449 nm, Se: 523 nm, and Te: 610 nm) with bent structures, suggesting strong interactions between each of the C–Ch multiple bonds due to their bent structures.[41–43] And, the λ_{max} value of 1_{Sn} is red-shifted relative to those of 1_{Ge} [265 nm (ε 11 000 dm³ mol⁻¹ cm⁻¹), 272 nm (ε 12 000 dm³ mol⁻¹ cm⁻¹), and 283 nm (ε 11 000 dm³ mol⁻¹ cm⁻¹)] and tetrakis(trimethylsilyl)allene[32,33] (273 nm, ε 36 000 dm³ mol⁻¹ cm⁻¹), indicating a narrowing of the HOMO–LUMO gap of 1_{Sn} relative to that of the germanium analogue 1_{Ge} due to the insufficient orbital overlap of 5pπ–2pπ in 1_{Sn} relative to that of 4pπ–2pπ in 1_{Ge} (Fig. S51†). Furthermore, the absorption maxima at 265–283 nm in 2-germapropadiene are expected to overlap with the π–π* transitions of phenyl groups. In contrast, the absorption peak of 2-stannapropadiene appears at 328 nm, which does not overlap with the π–π* transitions of phenyl

groups. Therefore, the epsilon value of 2-stannapropadiene is smaller than that of the germanium analogue. The UV-vis spectrum of 1_{Sn} in THF at room temperature exhibited a pronounced shoulder peak at 430 nm, which can be attributed to the coordination of a THF molecule to the central tin atom of 1_{Sn} (Fig. S56†). However, at 50 °C, the shoulder peak at 430 nm disappeared due to the dissociation of the coordinated THF molecule. Similarly, when donor molecules such as pyridine and 4-dimethylaminopyridine (DMAP) were added to a benzene solution of 1_{Sn}, similar shoulder peaks were observed in the respective spectra (Fig. S55†). Time-dependent density functional theory (TD-DFT) calculations were performed for compounds 1_{Sn} and $1_{Sn}\cdot$donor at the B3PW91/Def2tzvp level for Sn and the 6–311++G(2d,p) level for all other atoms. The results indicate a mixture of two π–π* transitions, i.e., one at 333 nm ($f = 0.0178$) and another at 306 nm ($f = 0.1589$), which is in good agreement with the observed λ_{max} value for 1_{Sn}. For $1_{Sn}\cdot$THF, the calculations suggested a mixture of two π–π* transitions associated with the bent allene moiety, whereby one occurs at 443 nm ($f = 0.0067$), consistent with the experimentally observed λ_{max} value. According to the theoretical calculations, the coordination of the donor molecule to 1_{Sn} to form $1_{Sn}\cdot$donor (donor: THF, pyridine, or DMAP) is expected to be exothermic for all cases except for THF (for details, see Table S52†). While the coordination of the donor molecule THF to the central tin atom of 1_{Sn} is endothermic, it is still likely that THF coordinates to the central tin atom in solution. The coordinated molecules of THF readily dissociate upon solvent distillation to regenerate 1_{Sn}. Recrystallization in the presence of THF or DMAP leads to the formation of 1_{Sn}, indicating that the coordination of these donors to 1_{Sn} in the crystalline solid state is not favorable. The higher positive charge on the central tin atom in 1_{Sn}, coupled with its lower steric demand compared to that of germanium derivative 1_{Ge}, suggests a preference for the coordination of donor molecules to the central tin atoms.

The reaction of 1_{Sn} with H_2O immediately produces stannadiol 2 (Scheme 2). Subsequently, the reaction of 1_{Sn} with 2 eq. of MeLi followed by H_2O affords the corresponding dimethylated compound 3. As expected, 1_{Sn} readily reacts with hydrogen chloride under mild conditions to quantitatively form the corresponding dichlorostannane (4Cl). These reactivity patterns are similar to those of 2-germapropadiene (1_{Ge}), indicating that the central tin atom can be expected to be the most electrophilic atom in the C=Sn=C allene moiety. In order to further explore the reactivity of 1_{Sn}, we undertook an investigation involving the reaction between 1_{Sn} and the $SnX_2\cdot$dioxane complex. This reaction was motivated by our previous syntheses of four-membered cyclic compounds derived from bis(methylene)-λ⁴-chalcogenanes using $GeX_2\cdot$dioxane (X = Cl, Br).[43] The reaction of 1_{Sn} with $SnX_2\cdot$dioxane proceeded smoothly even at room temperature to afford the corresponding four-membered stannylenes (5X) as light brown solids, which are thermally stable but sensitive to H_2O, which selectively affords decomposed 4X.

The experimental molecular structure and theoretical calculations suggest that 5Cl contains a Sn^{2+} and a Sn^{4+} atom (Fig. 6). The shortest distance between divalent tin atoms in 5Cl is 7.20 Å, which indicates that 5Cl is monomeric in the solid

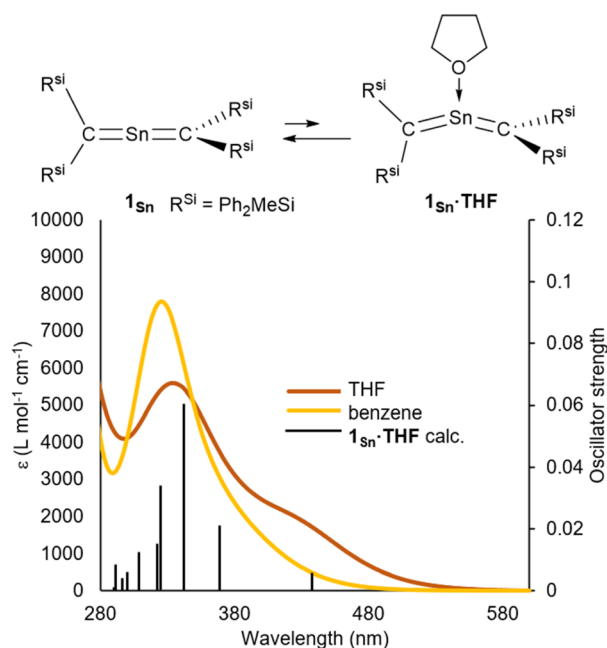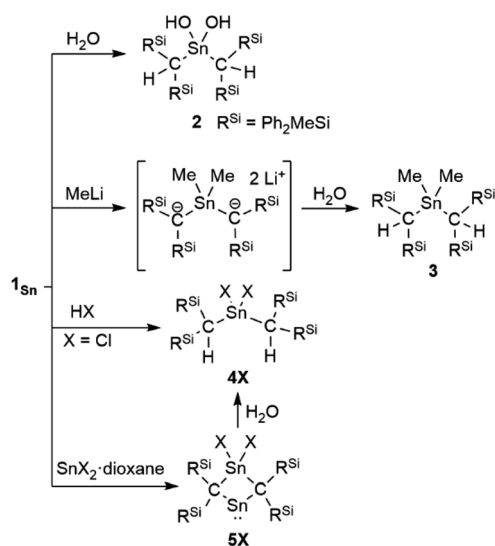Fig. 5 (a) UV-vis spectra of 1_{Sn} in benzene and THF at room temperature, and simulated UV-vis absorption spectrum of $1_{Sn}\cdot$THF obtained from TD-DFT calculations, together with theoretical oscillator-strength values (black vertical lines).

Scheme 2 Reactivity patterns of 1_{Sn}.

state. In contrast, there is a weak intermolecular interaction between Sn1⋯Sn2 in **5Cl** (3.1022(5) Å), which is shorter than the sum of the van der Waals radii (4.34 Å).[44] The Sn1 center adopts a typical di-coordinated Sn^{2+} geometry, and the Sn2 center shows a typical tetra-coordinated Sn^{4+} geometry. The C1–Sn1–C2 bond angle of **5Cl** (87.93(5)°) is similar to that of a previously reported five-membered dialkylstannylene (86.7(2)°).[38] The Sn1–C bonds in **5Cl** (2.313(2) Å and 2.300(2) Å) are significantly longer than those of a hitherto reported dialkylstannylene (2.218(7) Å and 2.223(7) Å), indicating small amounts of strain due to the four-membered ring in **5Cl**. The bond length of Sn2–C (2.163(2) Å and 2.173(2) Å) is identical to that of typical Sn–C bonds (2.16 Å), indicating an increased p-character of the central Sn^{2+} atom in the Sn1–C single bonds
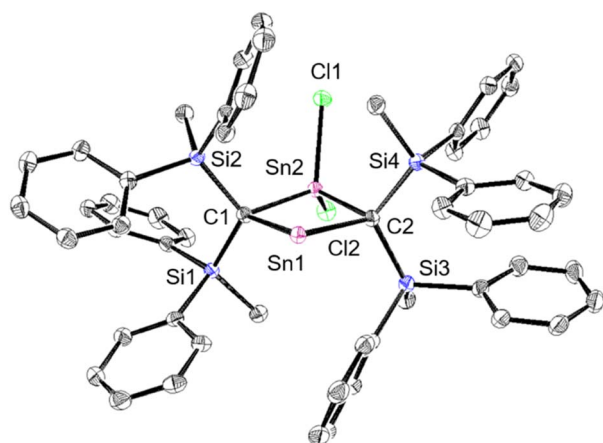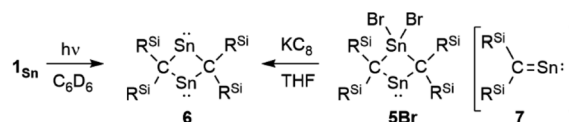

Fig. 6 Molecular structure of **5Cl** in the crystalline state with thermal ellipsoids at 50% probability; hydrogen atoms are omitted for clarity. Selected bond lengths [Å] and angles [°] for **5Cl**: Sn1⋯Sn2: 3.1022(5), C1–Sn1: 2.313(2), C2–Sn1: 2.301(2), C1–Sn2: 2.163(2), C2–Sn2: 2.173(2), C1–Si1: 1.905(2), C1–Si2: 1.888(2), C2–Si3: 1.902(2), C2–Si4: 1.909(2), C1–Sn1–C2: 87.93(8), C1–Sn2–C2: 95.22(8), Sn1–C1–Sn2: 87.67(8), and Sn1–C2–Sn2: 78.76(8).

in **5Cl** relative to that in 1_{Sn}. The four-membered ring of **5** deviates slightly from planarity (sum of the interior angles: 358.58°). The molecular structure of **5Br** is isostructural to that of **5Cl** (Fig. S43†). In the ^{1}H, ^{13}C, and ^{29}Si NMR spectra of **5X** in C_6D_6 at room temperature, a signal for only one set of silyl groups was observed, suggesting a flipping of the four-membered ring of **5X**. The ^{119}Sn NMR spectrum of **5Cl** in C_6D_6 exhibits signals at 1355 ppm for the Sn^{2+} nucleus and at 61 ppm for the Sn^{4+} nucleus. The signal for the Sn^{2+} nucleus of **5Cl** is shifted upfield relative to those of the kinetically stabilized stannylenes (**I**: 2323 ppm; **J**: 2299 ppm; Fig. 4),[38,39] indicating some kind of interaction with the Sn^{2+} nucleus. Unfortunately, the ^{119}Sn NMR spectrum of **5Br** could not be recorded due to prohibitively low solubility. To investigate the interactions with Sn^{2+}, NBO calculations were conducted at the B3PW91-D3(bj)/Def2tzvp level for Sn and the 6-311+G(2d,p) level for all other atoms. The vacant p orbital of Sn^{2+} in **5X** receives electron donation not only from the C–Si σ-bonds but also from the C–Sn^{4+} bonds, X–Sn^{4+} bonds, and π orbitals of the phenyl groups. This would increase the electron density on Sn^{2+}, resulting in a significant upfield shift of the [119]Sn signal of **5Cl**. In Fig. S28,† the UV-vis spectra of **5X** in benzene show absorption maxima at λ_{max} = 466 nm for **5Cl** (ε 1300 dm[3] mol^{−1} cm^{−1}) and λ_{max} = 472 nm for **5Br** (ε 1300 dm[3] mol^{−1} cm^{−1}), which are slightly blue-shifted compared to that of the five-membered cyclic stannylene **I** (484 nm; ε 400 dm[3] mol^{−1} cm^{−1}) in Fig. 4. Moreover, the absorption coefficients of **5X** are significantly higher than that of **I**, suggesting an expansion between the phenyl moieties and the vacant p orbital of Sn^{2+} obtained from the DFT calculations on **5X**.

To investigate the photostability of 1_{Sn}, we carried out photoreactions in C_6D_6 under irradiation from a 100 W high-pressure mercury lamp (Fig. S36†). After 3 days, one of the products obtained in the photochemical reaction was the four-membered cyclic bis(stannylene) (**6**). The formation of **6** implies the generation of a stannavinylidene (**7**) via cleavage of the C= Sn bond in 1_{Sn} under irradiation. The reduction of **5Br** with KC$_8$ also afforded bis(stannylene) **6** as a purple solid in 26% yield (Scheme 3). The shortest intermolecular distance between the tin atoms in **6** (7.1223(4) Å) indicates that **6** is monomeric in the solid state (Fig. 7). The intramolecular Sn1⋯Sn1′ distance (3.311(1) Å) is similar to those of related four-membered cyclic tin analogues (3.132(2)–3.4413(2) Å) as shown in Fig. 8.[45–54] The Sn1–C bonds in **6** (2.281(2) Å/2.301(1) Å) are similar to those of **5Br** (2.289(5) Å/2.310(5) Å). The four-membered ring of **6** exhibits perfect planar geometry (sum of the interior angles: 360°). The NMR spectra of **6** suggested that **6** adopts a highly symmetric structure in a solution: the ^{1}H NMR spectrum in C_6D_6 exhibits one set of signals due to four equivalent Ph$_2$MeSi

Scheme 3 Photolysis of 1_{Sn} and reduction of **5Br**.
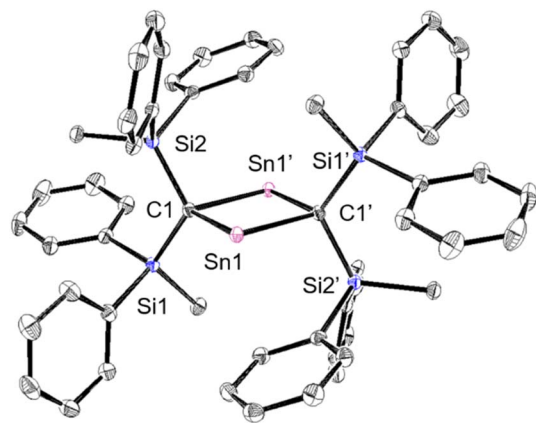
Fig. 7 Molecular structure of **6** in the crystalline state with thermal ellipsoids at 50% probability; hydrogen atoms are omitted for clarity. Selected bond lengths [Å] and angles [°] for **6**: Sn1···Sn1′: 3.311(1), C1–Sn1: 2.2812(13), C–Sn1′: 2.3015(14), C1–Si1: 1.8620(13), C1–Si2: 1.8707(13), C1–Sn1–C1′: 87.47(5), Sn1–C1–Sn1′: 92.53(5), and Si1–C1–Si2: 117.60(7).
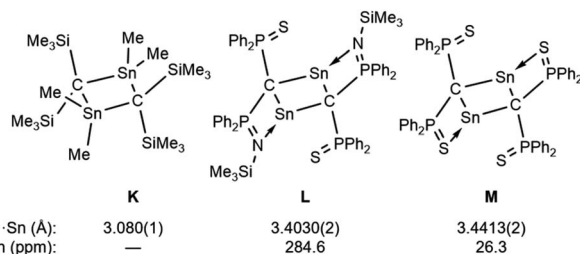

Fig. 8 Four-membered cyclic compound **K** and base-stabilized bis(-stannylene)s **L** and **M**.

groups, while the ^{119}Sn NMR spectrum of **6** shows only one signal at 2003 ppm. The chemical shift of the divalent tin nuclei in **6** is slightly upfield shifted compared to those of cyclic alkyl stannylenes **I** (2323 ppm)[38] and **J** (2299 ppm)[39] in Fig. 4, but significantly downfield shifted compared to that of precursor **5Cl** (1355 ppm) and those of base-stabilized bis(stannylene)s (284.6–(−11) ppm).[45–54]

The frontier Kohn–Sham orbitals of **6** provide further information on the nature of the divalent tin moieties (Fig. 9). The HOMO represents lone pairs on two tin atoms, while the LUMO
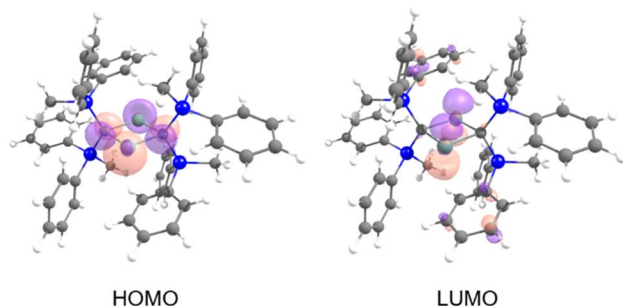

Fig. 9 Kohn–Sham orbitals of **6**.

consists of the vacant p orbitals on the tin atoms, indicating the typical molecular orbitals of a stannylene. The UV-vis spectrum of **6** in benzene exhibits an absorption maximum at $\lambda_{max} =$ 558 nm (ε 700 dm^3 mol^{-1} cm^{-1}). Further studies on the reactivity patterns of **6** are currently in progress.

Conclusions

We have reported the successful synthesis of the first stable 2-stannapropadiene (**1$_{Sn}$**) with a linear allene-type structure. The bulky silyl groups dominate the structural features and govern the stability of the 2-stannapropadiene due to the high steric demand and negative hyperconjugation by the silyl groups. A multinuclear NMR analysis of the linear heteroallene confirmed the unsaturated Sn^{4+} oxidation state of the central Sn atom. The reaction of **1$_{Sn}$** with SnX$_2$·dioxane afforded a four-membered cyclic stannylene (**5X**), indicating a unique reactivity that stands in contrast to that of a previously reported 2-germapropadiene. The photolysis of **1$_{Sn}$** afforded bis(stannylene) **6**, which is most likely obtained from the dimerization of stannavinylidene **7**. Further investigations into the reactivity of **1$_{Sn}$** and bis(stannylene) **6** are currently in progress in our laboratories.

Data availability

The datasets supporting this article have been uploaded as part of the ESI.†

Author contributions

The project was designed by K. S. The synthesis and characterization are conducted by T. A. All authors contributed to the writing of the manuscript.

Conflicts of interest

There are no conflicts to declare.

Acknowledgements

Notes and references

1 M. Wu, Y. He, L. Zhang, R. Wei, D. Wang, J. Liu, L. Leo Liu and G. Tan, *Eur. J. Inorg. Chem.*, 2022, **2022**, e202200413.
2 T. Koike, T. Nukazawa and T. Iwamoto, *J. Am. Chem. Soc.*, 2021, **143**, 14332–14341.

3 S. Yao, A. Kostenko, Y. Xiong, A. Ruzicka and M. Driess, *J. Am. Chem. Soc.*, 2020, **142**, 12608–12612.

4 Y. Wang, M. Karni, S. Yao, A. Kaushansky, Y. Apeloig and M. Driess, *J. Am. Chem. Soc.*, 2019, **141**, 12916–12927.

5 T. Sugahara, T. Sasamori and N. Tokitoh, *Angew. Chem., Int. Ed.*, 2017, **56**, 9920–9923.

6 Y. Xiong, S. Yao, S. Inoue, J. D. Epping and M. Driess, *Angew. Chem., Int. Ed.*, 2013, **52**, 7147–7150.

7 K. C. Mondal, H. W. Roesky, M. C. Schwarzer, G. Frenking, B. Niepötter, H. Wolf, R. Herbst-Irmer and D. Stalke, *Angew. Chem., Int. Ed.*, 2013, **52**, 2963–2967.

8 P. K. Majhi and T. Sasamori, *Chem.–Eur. J.*, 2018, **24**, 9441–9455.

9 J. Xu, C. Dai, S. Yao, J. Zhu and M. Driess, *Angew. Chem., Int. Ed.*, 2022, **61**, e202114073.

10 J. Xu, S. Pan, S. Yao, G. Frenking and M. Driess, *Angew. Chem., Int. Ed.*, 2022, **61**, e202209442.

11 G. E. Miracle, J. L. Ball, D. R. Powell and R. West, *J. Am. Chem. Soc.*, 1993, **115**, 11598–11599.

12 B. E. Eichler, D. R. Powell and R. West, *Organometallics*, 1998, **17**, 2147–2148.

13 N. Tokitoh, K. Kishikawa and R. Okazaki, *Chem. Lett.*, 1998, **27**, 811–812.

14 B. Eichler and R. West, in *Advances in Organometallic Chemistry*, Academic Press, 2000, vol. 46, pp. 1–46.

15 B. E. Eichler, G. E. Miracle, D. R. Powell and R. West, *Main Group Met. Chem.*, 1999, **22**, 147–162.

16 B. E. Eichler, D. R. Powell and R. West, *Organometallics*, 1999, **18**, 540–545.

17 M. Trommer, G. E. Miracle, B. E. Eichler, D. R. Powell and R. West, *Organometallics*, 1997, **16**, 5737–5747.

18 K. Sugamata and T. Sasamori, *Dalton Trans.*, 2023, **52**, 9882–9892.

19 L. Baiget, H. Ranaivonjatovo, J. Escudié and H. Gornitzka, *J. Am. Chem. Soc.*, 2004, **126**, 11792–11793.

20 C. Foo, K.-C. Lau, Y.-F. Yang and C.-W. So, *Chem. Commun.*, 2009, 6816–6818.

21 W.-P. Leung, Y.-C. Chan and T. C. W. Mak, *Inorg. Chem.*, 2011, **50**, 10517–10518.

22 Y.-F. Yang, C. Foo, H.-W. Xi, Y. Li, K. H. Lim and C.-W. So, *Organometallics*, 2013, **32**, 2267–2270.

23 K. Sugamata, T. Asakawa, D. Hashizume and M. Minoura, *Angew. Chem., Int. Ed.*, 2023, **62**, e202302836.

24 A. Inoue, J. Kondo, H. Shinokubo and K. Oshima, *Chem. Lett.*, 2001, **30**, 956–957.

25 R. C. Fischer and P. P. Power, *Chem. Rev.*, 2010, **110**, 3877–3923.

26 H. Meyer, G. Baum, W. Massa, S. Berger and A. Berndt, *Angew. Chem., Int. Ed.*, 1987, **26**, 546–548.

27 G. Anselme, H. Ranaivonjatovo, J. Escudie, C. Couret and J. Satge, *Organometallics*, 1992, **11**, 2748–2750.

28 Y. Mizuhata, N. Takeda, T. Sasamori and N. Tokitoh, *Chem. Commun.*, 2005, 5876–5878.

29 A. Fatah, R. El Ayoubi, H. Gornitzka, H. Ranaivonjatovo and J. Escudié, *Eur. J. Inorg. Chem.*, 2008, **2008**, 2007–2013.

30 R. Bashkurov, N. Fridman, D. Bravo-Zhivotovskii and Y. Apeloig, *Chem.–Eur. J.*, 2023, **29**, e202302678.

31 E. D. Glendening, C. R. Landis and F. Weinhold, *J. Comput. Chem.*, 2019, **40**, 2234–2241.

32 R. West and P. C. Jones, *J. Am. Chem. Soc.*, 1969, **91**, 6156–6161.

33 A. de Meijere, D. Faber, U. Heinecke, R. Walsh, T. Müller and Y. Apeloig, *Eur. J. Org Chem.*, 2001, **2001**, 663–680.

34 C. Kaiya, K. Suzuki and M. Yamashita, *Angew. Chem., Int. Ed.*, 2019, **58**, 7749–7752.

35 Y. Mizuhata, N. Noda and N. Tokitoh, *Organometallics*, 2010, **29**, 4781–4784.

36 Y. Mizuhata, T. Sasamori, N. Takeda and N. Tokitoh, *J. Am. Chem. Soc.*, 2006, **128**, 1050–1051.

37 Y. Mizuhata, N. Takeda, T. Sasamori and N. Tokitoh, *Chem. Lett.*, 2005, **34**, 1088–1089.

38 M. Kira, R. Yauchibara, R. Hirano, C. Kabuto and H. Sakurai, *J. Am. Chem. Soc.*, 1991, **113**, 7785–7787.

39 C. Eaborn, M. S. Hill, P. B. Hitchcock, D. Patel, J. D. Smith and S. Zhang, *Organometallics*, 2000, **19**, 49–53.

40 N. Wiberg, H.-W. Lerner, S.-K. Vasisht, S. Wagner, K. Karaghiosoff, H. Nöth and W. Ponikwar, *Eur. J. Inorg. Chem.*, 1999, 1211–1218.

41 K. Sugamata, T. Asakawa, Y. Urao and M. Minoura, *Inorg. Chem.*, 2022, **61**, 17641–17645.

42 K. Sugamata, Y. Urao and M. Minoura, *Chem. Commun.*, 2019, **55**, 8254–8257.

43 K. Sugamata, D. Hashizume, Y. Suzuki, T. Sasamori and S. Ishii, *Chem.–Eur. J.*, 2018, **24**, 6922–6926.

44 M. Mantina, A. C. Chamberlin, R. Valero, C. J. Cramer and D. G. Truhlar, *J. Phys. Chem. A*, 2009, **113**, 5806–5812.

45 W.-P. Leung, Y.-C. Chan and T. C. W. Mak, *Organometallics*, 2013, **32**, 2584–2592.

46 W.-P. Leung, W.-K. Chiu and T. C. W. Mak, *Inorg. Chem.*, 2013, **52**, 9479–9486.

47 W.-P. Leung, K.-W. Kan and T. C. W. Mak, *Organometallics*, 2010, **29**, 1890–1896.

48 W.-P. Leung, C.-L. Wan, K.-W. Kan and T. C. W. Mak, *Organometallics*, 2010, **29**, 814–820.

49 P. B. Hitchcock, M. F. Lappert, M. Linnolahti, J. R. Severn, P. G. H. Uiterweerd and Z.-X. Wang, *J. Organomet. Chem.*, 2009, **694**, 3487–3499.

50 W.-P. Leung, K.-W. Wong, Z.-X. Wang and T. C. W. Mak, *Organometallics*, 2006, **25**, 2037–2044.

51 W.-P. Leung, Q. W.-Y. Ip, S.-Y. Wong and T. C. W. Mak, *Organometallics*, 2003, **22**, 4604–4609.

52 W. P. Leung, Z. X. Wang, H. W. Li, Q. C. Yang and T. C. Mak, *J. Am. Chem. Soc.*, 2001, **123**, 8123–8124.

53 W.-P. Leung, Z.-X. Wang, H.-W. Li and T. C. W. Mak, *Angew. Chem., Int. Ed.*, 2001, **40**, 2501–2503.

54 N. Wiberg, T. Passler, S. Wagner and K. Polborn, *J. Organomet. Chem.*, 2000, **598**, 292–303.